processes

MDPI

Article

The Influence of High-Pressure Water Jet Cutting Parameters on the Relief of Pressure around the Coal Slot

Zuo Sun [1], Yingjie Liu [1], Qingjie Qi [1], Jiamei Chai [1,*] and Beifang Gu [2]

[1] Emergency Science Research Institute, Chinese Institute of Coal Science, Beijing 100013, China; sunzuo@mail.ccri.ccteg.cn (Z.S.); liuyingjie@mail.ccri.ccteg.cn (Y.L.); qiqingjie@mail.ccri.ccteg.cn (Q.Q.)
[2] School of Environmental and Municipal Engineering, North China University of Water Resources and Electric Power, Zhengzhou 450045, China; gubeifang@ncwu.edu.cn
* Correspondence: chaijiamei@mail.ccri.ccteg.cn

Abstract: This research aims to investigate the impact of high-pressure water jet cutting parameters on pressure alleviation around the coal slot. A numerical model of high-pressure water jet cutting coal was developed using FLAC^{3D} software, allowing for a detailed study of how each cutting parameter affects the pressure relief effect of the slot. The key findings are as follows: as the water jet pressure increases, the plastic area of the coal body around the kerf expands, although the rate of increase diminishes, with the optimal water jet pressure being 30 Mpa. The results suggest that hydraulic slotting measures are particularly beneficial for outburst prevention in high in situ stress coal seams. The pressure relief range exponentially grows with an increase in the kerf depth, signifying that enhancing the kerf depth has a notable effect on improving the hydraulic kerf pressure relief. As the slit width increases, the volume of the slit enlarges, leading to a significant rise in the pressure relief range of the surrounding coal body. Given that an increase in the slit width necessitates an increase in the nozzle outlet diameter and slotting time, the optimal slit width is determined to be 0.2 m. The research concludes that the optimal hydraulic slit spacing is 3 m. This study offers valuable theoretical guidance for high-pressure water jet slotting.

Keywords: high-pressure water jet; pressure relief; FLAC^{3D}; slot parameters; in situ stress

check for updates

Citation: Sun, Z.; Liu, Y.; Qi, Q.; Chai, J.; Gu, B. The Influence of High-Pressure Water Jet Cutting Parameters on the Relief of Pressure around the Coal Slot. *Processes* **2023**, *11*, 2071. https://doi.org/10.3390/pr11072071

Academic Editors: Feng Du, Aitao Zhou and Bo Li

Received: 24 May 2023
Revised: 4 July 2023
Accepted: 7 July 2023
Published: 11 July 2023

Copyright: © 2023 by the authors. Licensee MDPI, Basel, Switzerland. This article is an open access article distributed under the terms and conditions of the Creative Commons Attribution (CC BY) license (https://creativecommons.org/licenses/by/4.0/).

1. Introduction

Coal is the main energy source in China. In recent years, with the increase in mining depth, the gas content in low-permeability coal seams has gradually increased, resulting in low gas drainage efficiency and poor effects [1,2]. Various measures can enhance coal seam permeability to address mining challenges technically. Improving the coal seam's permeability enhances gas circulation, thus boosting the coal seam's gas drainage effect to prevent outbursts [3,4]. For coal exhibiting poor gas permeability, an array of effective technical methods can be employed to augment coal's gas permeability [5–7]. Various efficacious strategies and methods can be distilled from domestic and international practice, such as mining protective layers and implementing various hydraulic measures, among others [8–14].

The hydraulic slotting technology uses high-pressure jet water as the medium to cut coal in a borehole to form a new slot, so as to increase the permeability of the coal seam and reduce the stress of the original rock coal seam, so as to form pressure relief and permeability enhancement effects on the surrounding coal and improve the gas drainage efficiency. Therefore, the application effect of hydraulic slotting for harder coal is significant, and hydraulic slotting is an effective outburst prevention measure [15].

Ye et al. investigated the mechanism of high-pressure abrasive hydraulic kerf anti-outburst technology, analyzed its technological process, and verified its beneficial application effect through experiments [16]. Kou et al. conducted a comparable simulation experiment to determine the nozzle rotation parameters when hydraulic kerf was utilized

for pressure relief and permeability enhancement in the coal seam [17]. Chen examined the anti-outburst mechanism and corresponding supportive equipment of the integrated construction of drilling and hydraulic slotting technology, applying it on-site [18]. Liu et al. evaluated the effects of different slotting techniques, analyzed the impact of progressive and regressive hydraulic slotting on the pressure relief and permeability enhancement of coal seams, and proposed slotting techniques suitable for different mining conditions [19]. Yi et al. studied the pressure relief effect of a high-pressure water jet fracturing coal through a theoretical analysis, analogous experiments, and numerical simulation, and analyzed the pressure relief law with various cutting parameters [20]. Zhang et al. acquired a theoretical model of the annular kerf depth of the high-pressure water jet through theoretical modeling and field test validation [21]. Zhang et al. concluded, through theoretical analysis, numerical simulation, and field tests, that high-pressure water jets can cut annular slots in the coal seam to lessen the coal body's stress, thereby enhancing the coal seam's permeability and improving gas drainage [22]. Liu et al. designed a high-pressure rotary sealing device, demonstrating that a water jet can effectively reduce dust concentration when cutting rocks [23]. Xiao et al. examined the distribution of particle size, morphology, and fractal characteristics during coal crushing under high-pressure water jet cutting [24]. Zhou et al. established an elastoplastic damage numerical model based on the material point method, and simulated the effect of hydraulic slotting on pressure relief desorption and permeability enhancement of linking deep CBM [25]. Deng et al. used COMSOL Multiphysics multi field coupling software to carry out numerical simulation, and selected slotting radius, drainage time, gas pressure and permeability as the main influencing factors, analyzed the variation law of gas drainage radius under different influencing factors, and carried out field test [26].

Scholars have carried out a lot of research on the optimization measures and effects of hydraulic slotting but, due to the complexity of the coal mass's failure process, current research on the pressure relief failure effect on the surrounding coal mass, based on hydraulic kerf parameters, is inadequate. Taking Tanjiachong No.6 Coal Seam as an example, this study uses the method of numerical simulation and field engineering verification to analyze the influence of slotting parameters on the distribution of stress–strain and plastic regions of coal around the slot, obtain reasonable hydraulic slotting parameters, and determine the optimal spacing of hydraulic slotting in the working face. This study has important theoretical and engineering significance for improving the efficiency of hydraulic slotting and the effect of coal and rock pressure relief.

2. Numerical Model Construction

FLAC^{3D} was developed by ITASA in the United States, and is widely used for simulating the three-dimensional structural stress characteristics and plastic flow analysis of rocks and soil. FLAC^{3D} is solved by a three-dimensional fast Lagrange algorithm, including five kinds of solution models, which are the static model, dynamic model, creep model, seepage model and temperature model. Because mesh generation affects the simulation results, FLAC^{3D} has built-in automatic 3D mesh generator.

The FLAC^{3D} numerical model parameters were established according to the geological data of the Tanjiachong No.6 coal seam. The model, a cuboid, has dimensions of 17 m along the strike (X-axis), 10 m along the dip (Y-axis), and 17 m vertically (Z-axis). The model's grid sizes are 1 m, 1 m, and 0.05 m in the X, Z, and Y-axis directions, respectively. The drilling grid is cylindrical, with a set kerf depth of 1 m. The numerical calculation model is divided into 53,600 units. According to the site conditions, the working face direction in the model is set as the x-axis direction, and the working face inclination is set as the y-axis direction. In order to facilitate the observation of the slotted model, the slotted model is locally enlarged, as shown in Figure 1. The numerical model's material parameters are shown in Table 1.

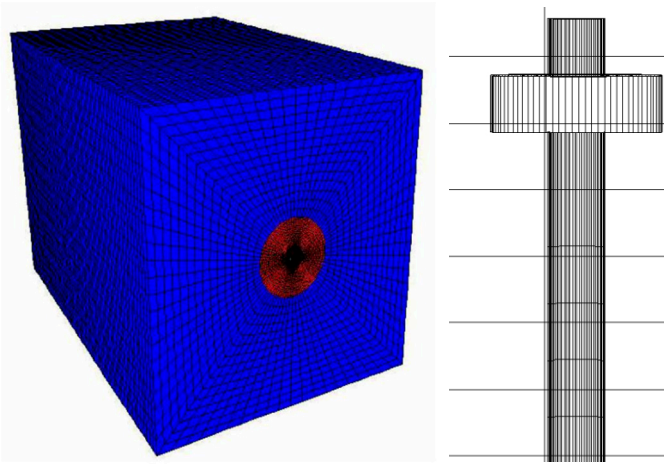


Figure 1. Numerical simulation model and hydraulic cutting model.

Table 1. The mechanical parameters in numerical simulation.

Shear Modulus *S*	Internal Friction Angle *F*	Bulk Modulus *B*	Density *D*	Tensile Strength *T*	Cohesion *C*
(Pa)	**(°)**	**(Pa)**	**(kg/m^3)**	**(Pa)**	**(Pa)**
0.19×10^9	20	0.36×10^9	1400	0.03×10^6	1×10^6

FLAC^{3D} has a variety of initial in situ stress field methods. According to the numerical simulation, in order to be simple and fast, the elastic solution method is selected. The specific steps of the elastic solution method are: first, set the model material as the elastic model, then set the shear modulus and volume modulus in the material parameters to the maximum value, which can prevent the plastic failure of the model during stress initialization, and finally apply the initial in situ stress field to the model.

The numerical simulation employs the Mohr–Coulomb constitutive model, with the calculation accuracy set to 10^{-5}. Maximum values are assigned to the shear modulus and bulk modulus in the material parameters, which prevent the model from initializing the stress. The stress nephogram following in situ stress initialization is presented in Figure 2.

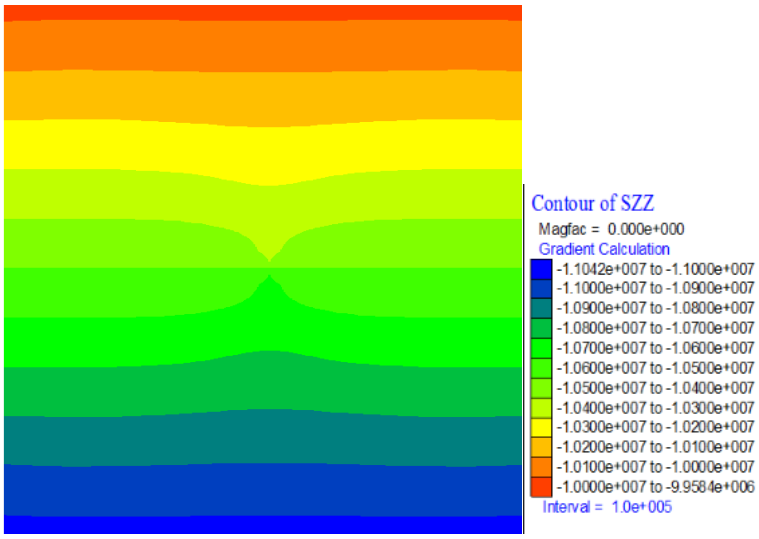


Figure 2. Initial stress field vertical stress state.

3. Simulation Results of Different Kerf Parameters

Various slotting parameters were selected for numerical simulation research. The chosen parameters include: nozzle outlet pressure P, in situ stress F, slit depth r, slit width d and slit spacing L. After the completion of numerical simulation, the deformation and plastic distribution nephogram under various working conditions is derived. The stress–strain and plastic region changes of coal around the slit are recorded through the nephogram, and the influence of different parameters on coal pressure relief is analyzed.

3.1. Simulation Analysis of Nozzle Outlet Pressure

Focusing on the water jet pressure's influence, the slit width was set to 0.2 m, the slit depth to 1 m, and pressure value gradients were chosen as 5 MPa, 10 MPa, 15 MPa, 20 MPa, 25 MPa, 30 MPa, 35 MPa, and 40 MPa, respectively, to examine coal stress–strain and plastic failure states.

Figure 3 displays the stress cloud diagram of the coal body surrounding the slit in the Y direction under varying water jet pressures. The area far from the slit maintains its original stress state. In the numerical model, as the impact force of the water jet applied by the nozzle on the bottom of the slot gradually increases, the stress unloading of the coal body around the slot likewise increases in all directions. Under various pressure gradients, stress unloading in the Y direction is greater than in the other two directions, and is proportional to the pressure gradient. As the water jet pressure increases, the high-stress area in the coal body gradually shifts towards the deeper part, thereby achieving pressure relief. This indicates that increasing the water jet pressure is an effective method to augment the pressure relief range of the slot.

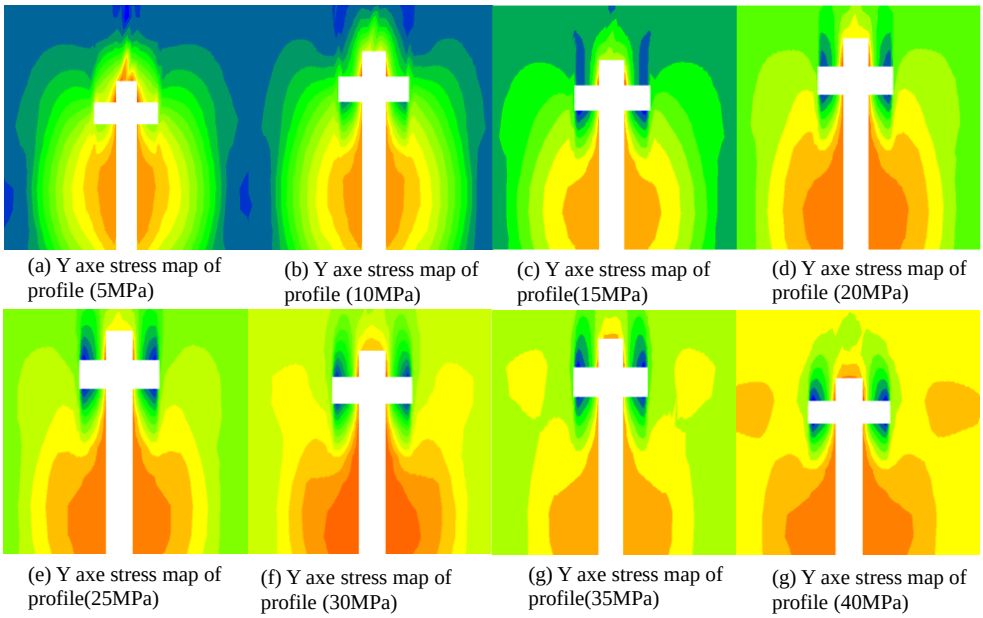


Figure 3. Y axe stress map of profile.

As depicted in Figure 4, the displacement cloud map of the coal mass surrounding the slit in the Y direction under varying pressure gradients at the water jet nozzle outlet was analyzed. As discerned from the figure, deformation towards the kerf is observed on either side following hydraulic slotting, and the nodes' displacement on both kerf sides incrementally increases with rising water jet pressure. The displacement contrasts on either kerf side are approximately symmetrical, but in opposing directions. With a nozzle outlet pressure of 5 MPa, the coal body's maximum displacement in the Y direction is 8.5 mm, and this maximum displacement increases as the nozzle outlet pressure gradient rises. By tracking the maximum displacement change, a curve portraying the maximum displacement of the coal mass around the seam versus the nozzle outlet pressure gradient

is plotted in Figure 5. As can be inferred from the figure, the relationship between the two is nearly proportional, indicating that the pressure relief effect of hydraulic cutting can be notably improved by increasing the water jet pressure.

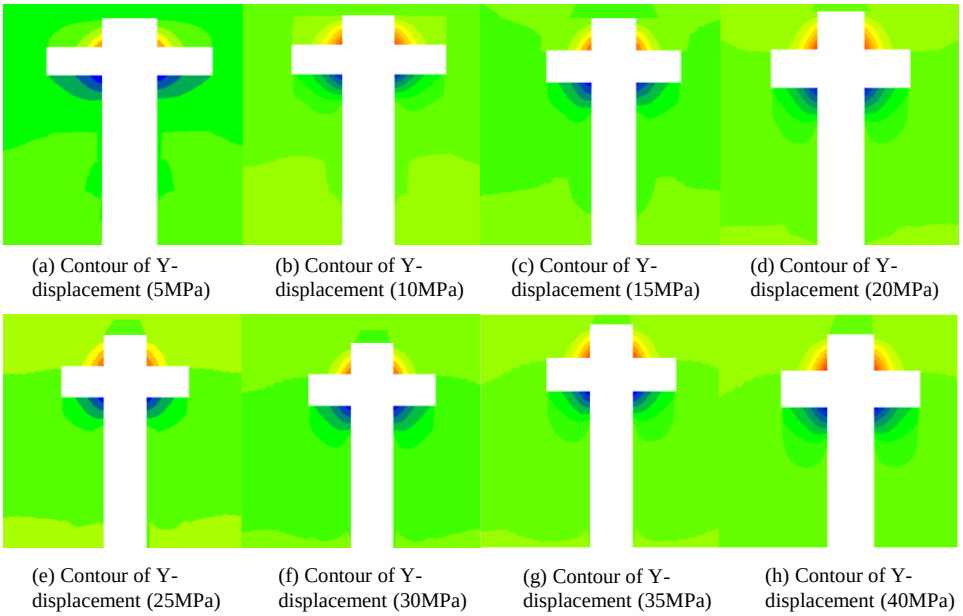


Figure 4. Contour of Y-displacement.

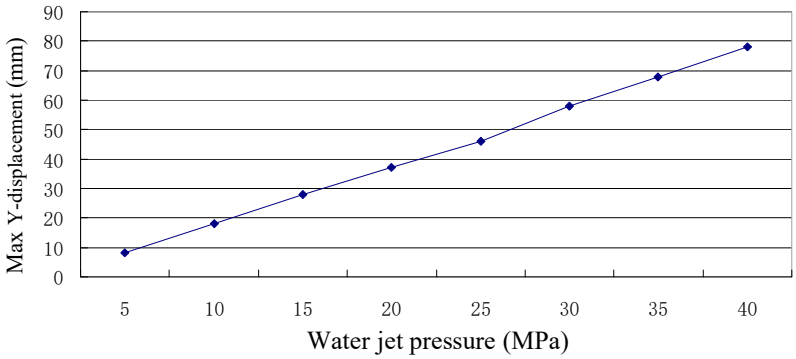


Figure 5. Contour of max Y-displacement with different water jet pressure.

Figure 6 illustrates the area where the coal mass around the slit reaches the current yield surface under different water jet pressures. It is evident from the figure that, as water jet pressure persistently increases from 5 MPa to 40 MPa, the plastic region of the coal mass around the cut enlarges, and the pressure gradient between the coal mass around the cut and the nozzle outlet water pressure does not follow a simple linear relationship. As shown in Figure 6, it can be observed that, when the nozzle outlet pressure escalates from 5 MPa to 30 MPa, the coal mass area surrounding the slit in the current plastic region increases rapidly, whereas it increases more slowly from 30 MPa to 40 MPa. Given the complications related to safety and maintenance when hydraulic slotting equipment operates at excessively high water jet pressures, it is recommended that the water jet pressure be set to around 30 MPa to ensure an extensive influence range and economical operation. Consequently, the hydraulic slit's water jet pressure is set to approximately 30 MPa.

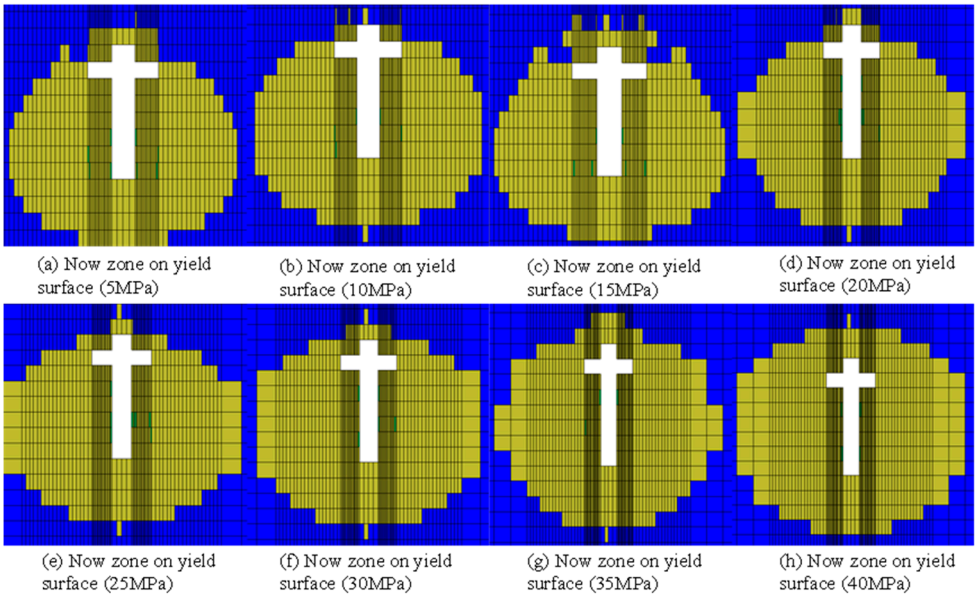


Figure 6. Now zone on yield surface.

3.2. Simulation Analysis of Ground Stress

Numerical simulation was conducted to assess the impact of ground stress, F represented by the depth of the coal seam. In situ stress comprises vertical stress σ_v and horizontal stress σ_h. Typically, the vertical stress σ_v is equivalent to the overlying coal strata's weight, represented as $\sigma_v = rH$. Horizontal stress encompasses two components: the maximum horizontal principal stress $\sigma_{h,max}$ and the minimum principal stress $\sigma_{h,min}$, with the approximate relationship between the two and burial depth given shown in Equation (1) [27]:

$$\begin{cases} \sigma_{h,\max} = 0.03H + 4.4 \\ \sigma_{h,\min} = 0.02H + 2.1 \end{cases} \quad (1)$$

In accordance with the site's actual conditions, the horizontal stress σ_h is chosen as the average value of the maximum horizontal principal stress $\sigma_{h,max}$ and the minimum principal stress $\sigma_{h,min}$, denoted as $\sigma_h = \frac{\sigma_{h,\max}+\sigma_{h,\min}}{2}$. Taking into account the actual situation, and calculation convenience, five burial depth gradients were established at 200 m, 400 m, 600 m, 800 m, and 1000 m, respectively. Other parameters were set as follows: kerf depth at 1 m, and kerf width at 0.2 m. Using Equation (1), the in situ stress values under different burial depths can be calculated, and are presented in Table 2.

Table 2. The mechanical parameters in numerical simulation.

Coal Seam Depth (m)	Vertical Stress σ_v (MPa)	Horizontal Stress σ_h (MPa)
200	5.2	8.0
400	10.5	13.0
600	15.7	17.9
800	20.9	22.7
1000	26.2	27.6

Figure 7 delineates the relationship between in situ stress (burial depth) and the maximum values of the plastic region and the maximum stress unloading in the X, Y and Z axes of the model. As the burial depth increases, as observed from the figure, the pressure relief range of the coal mass surrounding the kerf across the three coordinate axes also expands. The maximum value of stress unloading in all directions exceeds that of the plastic region, suggesting that, despite the absence of coal mass damage in these regions, stress reduction still occurs.

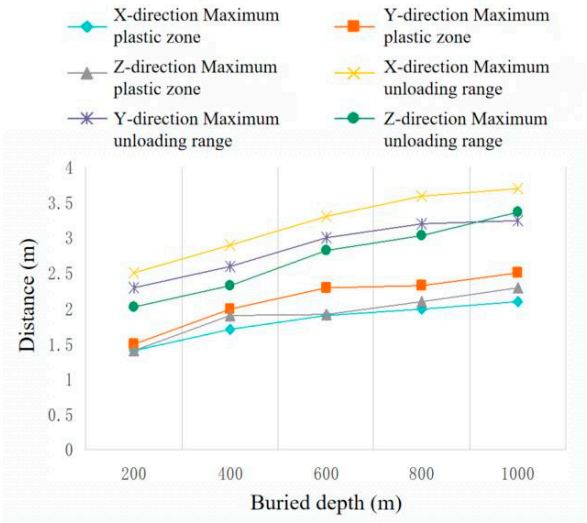


Figure 7. Relationship between buried depth and maximum unloading range.

The numerical simulation yields the stress unloading volume of the coal mass around the slot in all directions, and the correlation between the pressure unloading volume in each direction and the coal seam's burial depth is depicted in Figure 8. The figure reveals a similar trend in the stress unloading volume change of the coal mass around the slit in all directions, indicating an increase in the pressure unloading degree of the coal mass in the three axes with the rise in the coal seam depth. The stress unloading volume in the X direction is most affected by the buried depth of coal seam, followed by the Z direction, and finally the Y direction, but only the Z direction is not linear. This suggests that a deeper coal seam burial corresponds to higher in situ stress and a greater degree of pressure relief for the coal mass around the slot. This implies that in situ stress contributes to the pressure relief of the coal mass, and that the impact of hydraulic slotting measures is more pronounced in areas with high in situ stress.

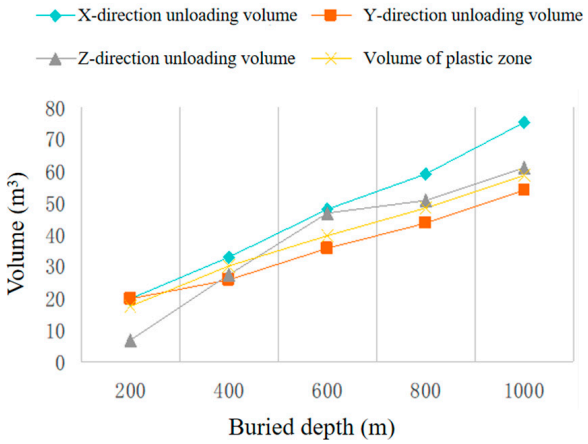


Figure 8. Relationship between buried depth and unloading volume of all directions.

Figure 9 presents the stress cloud diagram of the coal mass near the kerf in the Y direction under varying in situ stresses. As the in situ stress rises, the stress reduction area enlarges, and the pressure relief effect becomes more noticeable. This demonstrates that the increase in in situ stress widens the difference between the coal mass stress and the stress around the slot post-slotting. Additionally, when a new stress equilibrium is formed, the stress relief range also expands. Based on the above analysis, the greater the in situ stress, the more effective hydraulic cutting proves to be, indicating that hydraulic cutting technology is more suitable for outburst coal seams under large burial depth conditions.

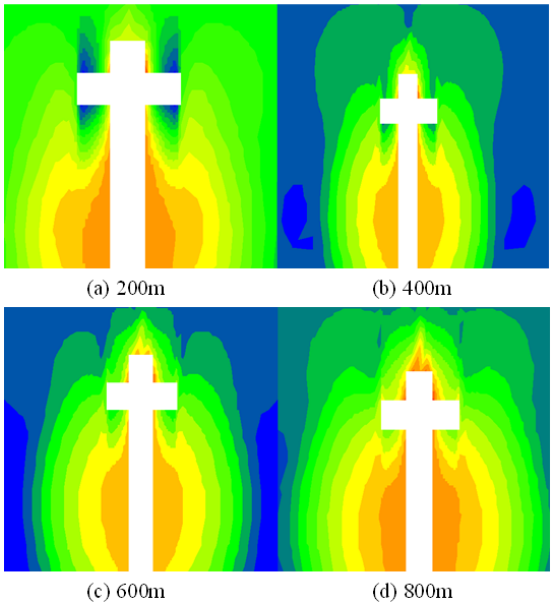


Figure 9. Contour of Y-stress at different ground stress.

3.3. Simulation Analysis of Kerf Depth

Kerf depths were set at 1 m, 1.5 m, 2 m, 2.5 m, and 3 m, respectively. Other parameters included a kerf width of 0.2 m, a water jet pressure of 30 MPa, and a coal seam burial depth of 400 m.

Figure 10a–e depicts the stress change cloud map of the coal mass around the slot in the Y direction under different slot depths. The region farther from the slot retains its original stress state. As kerf depth increases, the stress reduction area expands, and the magnitude of the stress reduction on either kerf side is essentially identical, but in opposite directions. For the kerf depth parameter, being significantly larger than the kerf width results in a greater degree of pressure relief in the Y direction than in other axes. Also, as the cutting depth increases, the coal area controlled by the hydraulic cutting measures expands, and the influence radius enlarges.

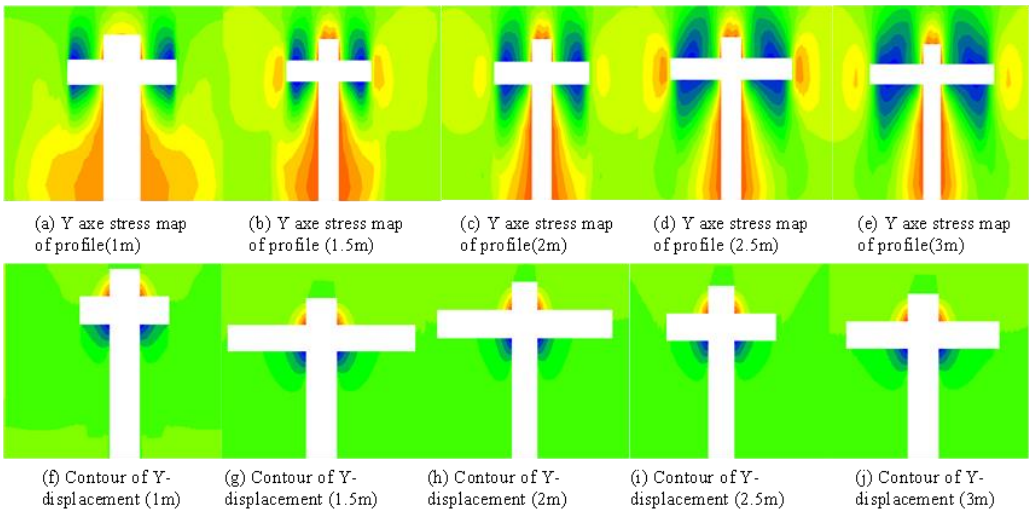


Figure 10. Y axis stress map of profile and contour of Y-displacement.

Figure 10f–j presents the displacement change diagram of the coal mass in the Y direction. Following hydraulic slotting, deformation towards the kerf is observed on both kerf sides, and as kerf depth increases, the nodes' displacement on either kerf side also

gradually rises. The displacement contrasts on either kerf side are roughly equal, but in opposite directions. This suggests that enhancing the kerf depth can improve the pressure relief effect of the hydraulic kerf.

Taking into account the practical circumstances on site, increasing the kerf depth necessitates a higher water pressure which, in turn, imposes more stringent equipment requirements. These conditions prove challenging to meet on site, and will result in a proportionate increase in kerf time. Therefore, the kerf depth cannot be infinitely increased; it must be determined in conjunction with field equipment conditions and field test data.

3.4. Simulation Analysis of Kerf Width

The kerf width was set in increments of 0.1 m, 0.2 m, 0.3 m, and 0.4 m. Other parameters include a kerf depth of 1 m, water jet pressure of 30 MPa, and a coal seam burial depth of 400 m. The stress–strain behavior of the coal mass around the slot and the failure state of the plastic region were investigated.

Figure 11 illustrates the stress change cloud map and displacement change cloud map of the coal mass around the slot in the Y direction under different slit widths. The slit width significantly influences the coal body's pressure relief. As the slot width increases, the degree of pressure relief for the coal mass around the slot is enhanced, and the stress unloading range of the coal mass widens. As more coal is removed, the slot's volume increases, thereby increasing the coal body's movement towards the slot and expanding the deformation and damage range of the coal body. This can effectively increase the contact area for gas migration, thereby enhancing the gas drainage effect. However, increasing the slit width requires a larger water jet nozzle outlet diameter and additional slotting time, which demands more advanced equipment, thus limiting the extent to which the slit width can be increased.

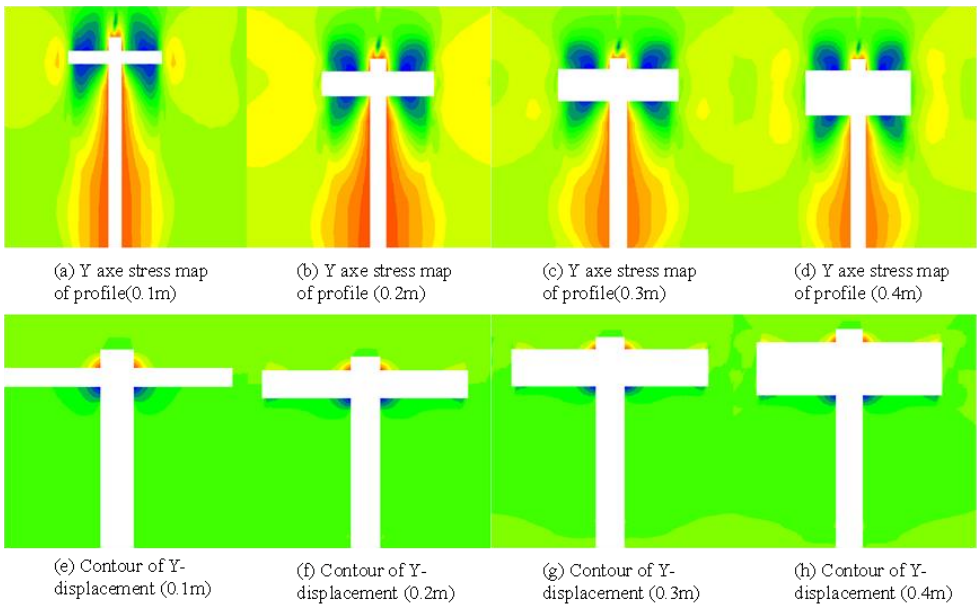


Figure 11. Y axis stress map of profile and contour of Y-displacement.

Figure 12 presents the extent of the plastic region of the coal mass around the kerf under different kerf widths. As the kerf width increases, the plastic region rapidly expands. When the kerf width is set to 0.1 m, the corresponding plastic failure area is 0.9 m. When the kerf width is set to 0.4 m, the plastic region expands to 3.4 m, exhibiting exponential growth. This suggests that increasing the slit width has a significant pressure relief effect on the surrounding coal body.

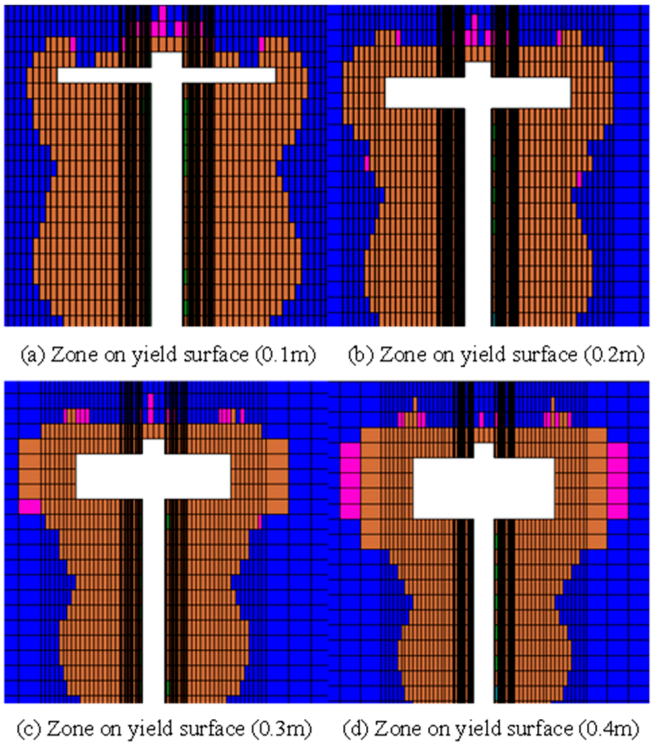


Figure 12. Zone on yield surface.

3.5. Simulation Analysis of Slot Spacing

The slot spacings were set at 2 m, 3 m, 4 m, and 5 m, respectively, with other parameters set as: a kerf depth of 1 m, a water jet pressure of 30 MPa, and a kerf width of 0.2 m. The assessment criteria were the stress–strain and plastic deformation regions between the two slots.

Figure 13 displays the stress change cloud map and displacement change cloud map of the coal body around the slot in the Y direction under different slot spacings. When the gap between the slots is relatively small, the coal mass between the slots undergoes repeated depressurization, and coal mass fissures are fully penetrated. As the slot spacing increases, the pressure relief overlap area between the slots gradually diminishes. When the gap between the slots widens to 4 m, an area in the middle of the two slots no longer undergoes repeated depressurization, and as the gap continues to expand, this area becomes more prominent. Moreover, the cloud map of the coal mass displacement between the slots reveals that as the spacing between the slots increases, the area with large displacement between the slots gradually shrinks until 5 m, at which point the coal mass in the middle of the slots is no longer affected by the slots on either side, leading to a suboptimal pressure relief effect in the coal seam.

The slot spacing significantly impacts the plastic deformation area of the coal mass between the slots. Figure 14, obtained by slicing the model, demonstrates the range of the plastic deformation area of the coal mass between slots under varying slot spacings. After the borehole is established, the surrounding coal mass undergoes plastic deformation. Following the construction of the water jet slit, this segment of the coal mass deforms again, resulting in a more pronounced pressure relief effect. There exists a recurring damage area in the coal mass between the slots. When the spacing between the slots extends to 4 m, a non-recurring damage area emerges between the slots, which adversely affects the pressure relief effect.

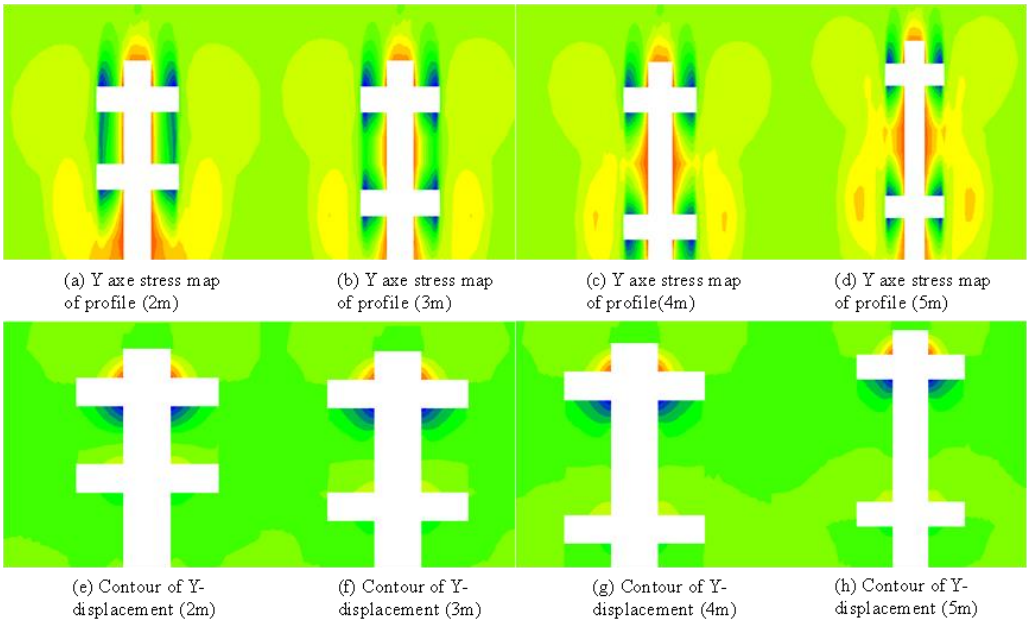


Figure 13. Y axis stress map of profile and contour of Y-displacement.

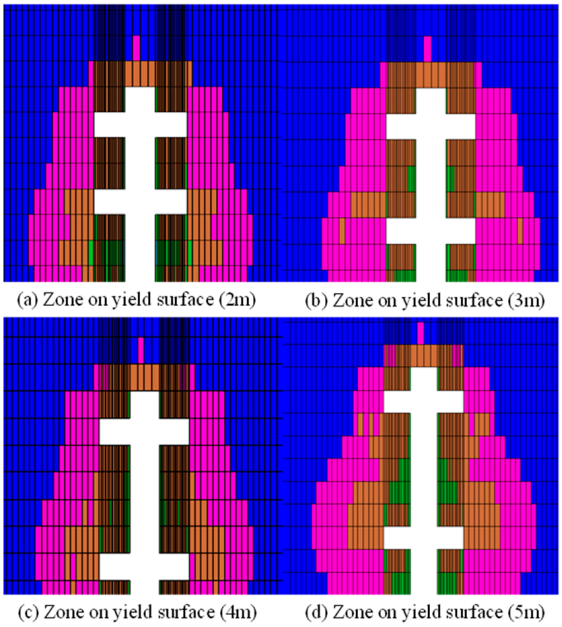


Figure 14. Zone on yield surface.

Based on these conclusions, it can be inferred that excessively close slot spacing impairs the stress unloading effect, leading to project inefficiencies. Therefore, in light of these research findings, it is proposed that the field application gap between the kerfs be set at 3 m, which satisfies the requirements for outburst prevention and project efficiency.

4. Field Validate

In order to verify the effectiveness of numerical simulation results, on-site experiments were conducted in the No.6 coal seam of Tanjiachong Coal Mine to determine the optimal spacing of hydraulic cutting seams.

4.1. Test Method

(1) Firstly, 8 investigation boreholes with a diameter of 75 mm are constructed. All the investigation boreholes are required to be parallel to each other, and the spacing of

boreholes is 1 m. The drilling arrangement is shown in Figure 15. For the extraction drilling with the same construction parameters, the hole shall be sealed immediately after the completion of construction, and the pressure gauge shall be connected to observe the pressure change;

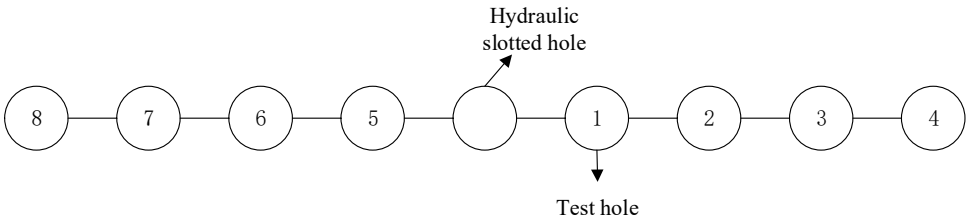


Figure 15. Sketch map of borehole.

(2) After the construction of all test holes is completed and the pressure gauge is stable, the hydraulic slotting drilling shall be constructed. After the completion of drilling construction, connect the hydraulic slotting drilling hole to the gas drainage system immediately, and regularly observe each test hole until the pressure is stable;

(3) After the gas pressure is stable, the hydraulic slotting operation shall be implemented. In order to solve the problem of borehole collapse and deformation, the casing hole is first carried out, and then the hydraulic cutting construction is carried out. After the construction is completed, the hole shall be sealed and the drainage shall be continued until the gas pressure in the test hole is stable. The basis for determining that the test hole is within the influence range of hydraulic cutting is that the gas pressure in the test hole is reduced by more than 10% compared with that before pre-drainage.

4.2. Test Results

The gas pressure changes of test holes 1–8 before and after the implementation of hydraulic slotting measures are counted, as shown in Figure 16.

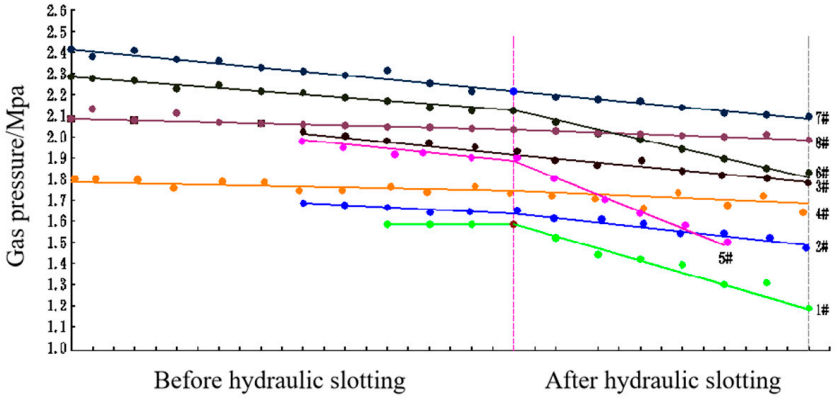


Figure 16. Gas pressure change of test boreholes.

As shown in Figure 16, there was a significant change in gas pressure during the construction of the hydraulic cutting measures for holes 1 and 5, resulting in a 35% decrease in gas pressure. The number of holes 2 and 6 decreased by 25%, while the number of holes 3 and 7 decreased slightly, but still reached 15%. According to the judgment basis, these test holes are all within the influence range of hydraulic cutting. The decrease in gas pressure in holes 4 and 8 is relatively small, about 5% and less than 10%, respectively.

Therefore, the optimal spacing of hydraulic slits determined in this experiment is between 3 m and 4 m. Considering redundancy, the optimal spacing of hydraulic slits is set at 3 m, which is consistent with the numerical simulation results.

5. Conclusions

A numerical model of a high-pressure water jet slotted coal mass was developed using FLAC^{3D}, and the impact of each slotting parameter on the slot's pressure relief effect was examined. The primary conclusions are as follows:

(1) With the steady rise in water jet pressure, the plastic area of the coal mass around the cut progressively enlarges. When the nozzle's water outlet pressure increases from 5 MPa to 30 MPa, the area of the coal mass around the cut within the plastic region rapidly expands, and the water outlet from the nozzle increases. When the pressure escalates from 30 MPa to 40 MPa, the plastic region's extent grows more slowly. Taking all factors into consideration, the optimal water jet pressure is 30 MPa;

(2) As vertical stress increases, the pressure relief range and damage range of the coal mass around the slot progressively enlarge, indicating that hydraulic slotting measures are particularly suitable for outburst elimination in coal seams with high in situ stress;

(3) As the kerf depth increases, the pressure relief range progressively expands, leading to an increased influence radius of the hydraulic kerf. The pressure relief range grows exponentially with the kerf depth, implying that increasing the kerf depth notably enhances the hydraulic kerf pressure relief effect;

(4) As the slit width increases, the volume of the slit enlarges, leading to a significant increase in the pressure relief range of the surrounding coal mass. However, considering that widening the slit requires increasing the nozzle outlet diameter and slotting time, the optimal slit width is determined to be 0.2 m;

(5) If the gap between the slits is too close, it affects the stress unloading effect and results in wasted resources. If the gap between the kerfs is too wide, a stress unloading blind spot emerges, which impairs the pressure unloading of the coal seam. When considering all factors, the optimal spacing for hydraulic slits and grooves is determined to be 3 m;

(6) Through field engineering tests, the optimal spacing of hydraulic cutting is determined to be 3 m, which verifies the results of numerical simulation.

Author Contributions: Methodology, investigation, writing—original draft, Z.S. and B.G.; formal analysis, conceptualization, writing—review and editing, Y.L. and Q.Q.; writing—review and editing, J.C. All authors have read and agreed to the published version of the manuscript.

Funding: The authors gratefully acknowledge the support provided by the National Natural Science Foundation of China (52204220, 52174188), and the China Coal Technology & Engineering Group Co., Ltd. (2022-QN001, 2023-TD-MS009).

Institutional Review Board Statement: Not applicable.

Informed Consent Statement: Not applicable.

Data Availability Statement: Not applicable.

Conflicts of Interest: The authors declare no conflict of interest.

References

1. Sun, Z.; Liu, Y.; Qi, Q.; Liu, W.; Li, D.; Chai, J. Risk Assessment of Coal Mine Flood Disasters Based on Projection Pursuit Clustering Model. *Sustainability* **2022**, *14*, 11131. [CrossRef]
2. Tang, Y.; Li, P.; Zhu, G. Application of ultra-high pressure hydraulic slotting technology in medium hardness and low permeability coal seam. *Coal Sci. Technol.* **2022**, *50*, 43–49.
3. Jiang, G.; Sun, M.; Fu, J. Research and application of complete set of technology for directional fracturing to increase coal seam permeability and eliminate coal/gas outbursts in underground coal mines. *China Coal* **2009**, *11*, 10–14.
4. Ma, X.; Li, Z.; Tu, H. Technology of deep-hole blasting for magnifying permeability in coal seam with high methane-content and low permeability. *Coalmining Technol.* **2010**, *1*, 92–93.
5. Duan, K.; Feng, Z.; Zhao, Y. Testing study of methane drainage by bore and hydraulic-cutting seam from low permeability coal seam. *J. China Coal Soc.* **2002**, *1*, 50–53.
6. Dong, G.; Lin, F. Experiment of high-pressure water jet reaming to improve pre-pumping effect of through-layer drilling. *Min. Saf. Environ. Prot.* **2001**, *3*, 17–18.

7. Gong, M.; Liu, W.; Wang, D.; Wu, H.; Qiu, D. Controlled blasting technique to improve gas pre-drainage effect in a coal mine. *J. Univ. Sci. Technol. Beijing* **2006**, *3*, 223–226.
8. Zhang, C.; Liu, Z.; Wang, B.; Li, L.; Zhu, X. Numerical simulation and test study on mechanical properties evolution of high-pressure water injection coal seam. *Chin. J. Rock Mech. Eng.* **2009**, *28*, 3371–3375.
9. Yu, B. *Technical Manual for Gas Disaster Prevention and Utilization*; China Coal Industry Publishing House: Beijing, China, 2005.
10. Guo, H. Theory and Technology of Underground Coal Mine Gas Drainage Based on Hydraulic Fracturing. Ph.D. Thesis, Henan Polytechnic University, Jiaozuo, China, 2010.
11. Zhang, G. Numerical Simulation of Hydraulic Fracturing in Horizontal Wells. Ph.D. Thesis, University of Science and Technology of China, Hefei, China, 2010.
12. Zarrouk, S.J.; Moore, T.A. Preliminary reservoir model of enhanced coalbed methane (ECBM) in a subbituminous coal seam, Huntly Coalfield, New Zealand. *Int. J. Coal Geol.* **2009**, *77*, 153–161. [CrossRef]
13. Liu, J.; Wang, H.; Yuan, Z.; Fan, X. Experimental Study of Pre-splitting Blasting Enhancing Pre-drainage Rate of Low Permeability Heading Face. *Procedia Eng.* **2011**, *26*, 818–823.
14. Tan, B.; He, J.; Pan, F. Application and analysis of deep hole pre-split blasting in low permeability and high outburst coal seam. *China Saf. Sci. J.* **2011**, *11*, 72–78.
15. Zhou, L.; Li, L.; Xia, B.; Yu, B. Study of fracture pattern and influencing factors of guided hydraulic fracturing with radial slot and well borehole. *J. China Coal Soc.* **2022**, *47*, 1559–1570.
16. Ye, Q.; Li, B.; Lin, B. Technology of high-pressure abrasive hydraulic cutting seam. *Saf. Coal Mines* **2005**, *12*, 13–16.
17. Kou, J.; Zhou, Z. Research on the influence of coal seam hydraulic slitting speed on the slit radius. *Coal Sci. Technol.* **2014**, *2*, 74–76.
18. Chen, L. Integrated technology of dual-power synergistic drilling and cutting coal and rock pressure relief, penetration enhancement and slitting. *Saf. Coal Mines* **2011**, *9*, 30–32.
19. Liu, F.; Huang, Y.; Xu, Q. Influence of advance and retreat high-pressure water jet slits on the effect of pressure relief and permeability enhancement in coal seam. *Saf. Coal Mines* **2014**, *9*, 165–168.
20. Yi, E.; Zhang, Y. Composite hazards prevention with breaking coal seam and roof by super high pressure water jet. *J. China Coal Soc.* **2021**, *46*, 1271–1279.
21. Zhang, Y.; Guo, S. Theoretical model of annular slotting depth for high pressure water jet and its application. *J. China Coal Soc.* **2019**, *44*, 126–132.
22. Zhang, Y.; Huang, Z.; Li, C. Investigation and application of high pressure water jet annularity slotting self pressure release mechanism. *J. China Coal Soc.* **2018**, *43*, 3016–3022.
23. Liu, S.; Ji, H.; Han, D.; Guo, C. Experimental investigation and application on the cutting performance of cutting head for rock cutting assisted with multi-water jets. *Int. J. Adv. Manuf. Technol.* **2018**, *94*, 2715–2728. [CrossRef]
24. Xiao, S.; Ge, Z.; Lu, Y.; Zhou, Z.; Li, Q. Investigation on Coal Fragmentation by High-Velocity Water Jet in Drilling: Size Distributions and Fractal Characteristics. *Appl. Sci.* **2018**, *8*, 1988. [CrossRef]
25. Zhou, L.; Peng, Y.; Lu, Y.; Xia, B. Numerical simulation of deep CBM hydraulic slotting pressure relief and desorption and permeability enhancement based on the MPM. *J. China Coal Soc.* **2022**, *47*, 3298–3309.
26. Deng, G.; Liu, W.; Li, G. Influence radius of hydraulic slotted hole drainage in low permeability coal seam. *J. Xi'an Univ. Sci. Technol.* **2022**, *42*, 619–628.
27. Jing, F.; Sheng, Q.; Yu, M. The change rule of the geostress and the elastic modulus of rock with depth and their mutual impact. In Proceedings of the 11th China Rock mechanics and Engineering Academic Conference, Wuhan, China; 2010; pp. 69–74.

Disclaimer/Publisher's Note: The statements, opinions and data contained in all publications are solely those of the individual author(s) and contributor(s) and not of MDPI and/or the editor(s). MDPI and/or the editor(s) disclaim responsibility for any injury to people or property resulting from any ideas, methods, instructions or products referred to in the content.